# Supporting Information

## Metzger et al. 10.1073/pnas.0904897106

### SI Text

**Structure Determination.** Data reduction was performed using XDS and XSCALE (1). The native structure was determined using the single anomalous wavelength method and the uranyl derivative dataset. Positions of uranium atoms were located using SHELXD (2) and utilized for phasing and density modification as implemented in SHARP/autoSHARP (3). The experimental electron density map was further improved using RESOLVE (4) and noncrystallographic symmetry averaging. The final experimental electron density map was sufficient for automatic chain tracing performed by ARP/wARP (5), which resulted in a partially complete model. This model was transferred to the high-resolution native dataset by using the rigid body refinement routine implemented in REFMAC (6). Model bias was prevented by rebuilding the model using ARP/wARP, which produced a model consisting of 837 residues. The model was completed through several cycles of manual building with COOT (7), followed by refinement with REFMAC. Water molecules were placed using ARP/wARP and manually checked with COOT. The final refinement step involved TLS parameterization (8) using 1 TLS group per protomer. The geometry of the final model was analyzed with PROCHECK (9) and SFCHECK (10) as implemented in ADIT (http://sw-tools.pdb.org). Figures were generated using POVscript+ (11) and POVRAY (http://povray.org) or PyMOL (http://www.delanoscientific.com).


1. Kabsch W (1993) Automatic processing of rotation diffraction data from crystals of initially unknown symmetry and cell constants. *J Appl Crystallogr* 26:795–800.
2. Sheldrick GM (2008) A short history of SHELX. *Acta Crystallogr A* 64:112–122.
3. Bricogne G, Vonrhein C, Flensburg C, Schiltz M, Paciorek W (2003) Generation, representation and flow of phase information in structure determination: Recent developments in and around SHARP 2.0. *Acta Crystallogr D* 59:2023–2030.
4. Terwilliger TC (2003) SOLVE and RESOLVE: Automated structure solution and density modification. *Methods Enzymol* 374:22–37.
5. Perrakis A, Morris R, Lamzin VS (1999) Automated protein model building combined with iterative structure refinement. *Nat Struct Biol* 6:458–463.
6. Murshudov GN, Vagin AA, Dodson EJ (1997) Refinement of macromolecular structures by the maximum-likelihood method. *Acta Crystallogr D* 53:240–255.
7. Emsley P, Cowtan K (2004) COOT: Model-building tools for molecular graphics. *Acta Crystallogr D* 60:2126–2132.
8. Winn MD, Murshudov GN, Papiz MZ (2003) Macromolecular TLS refinement in REFMAC at moderate resolutions. *Methods Enzymol* 374:300–321.
9. Laskowski RA, MacArthur MW, Moss DS, Thornton JM (1993) PROCHECK: A program to check the stereochemical quality of protein structures. *J Appl Crystallogr* 26:283–291.
10. Vaguine AA, Richelle J, Wodak SJ (1999) SFCHECK: A unified set of procedures for evaluating the quality of macromolecular structure-factor data and their agreement with the atomic model. *Acta Crystallogr D* 55:191–205.
11. Fenn TD, Ringe D, Petsko GA (2003) POVScript+: A program for model and data visualization using persistence of vision ray-tracing. *J Appl Crystallogr* 36:944–947.

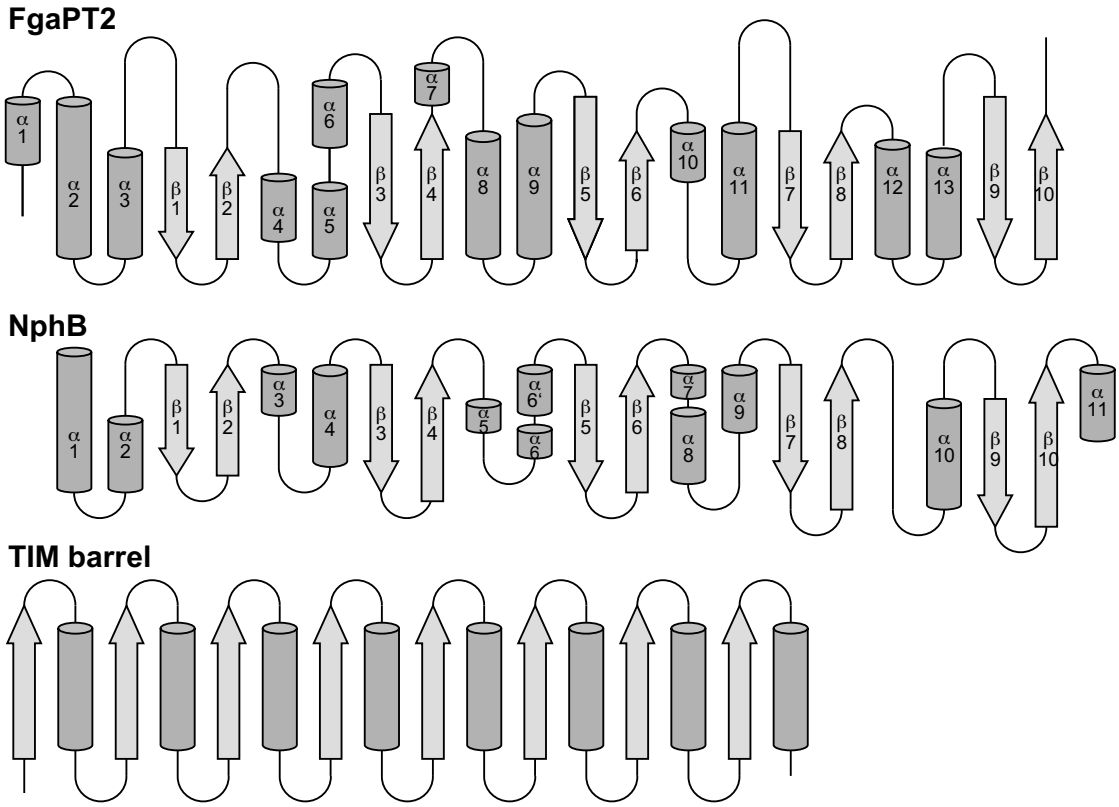


**Fig. S1.** Scheme of the secondary structure elements of the PT barrels of FgaPT2 and NphB and comparison with the TIM barrel fold.

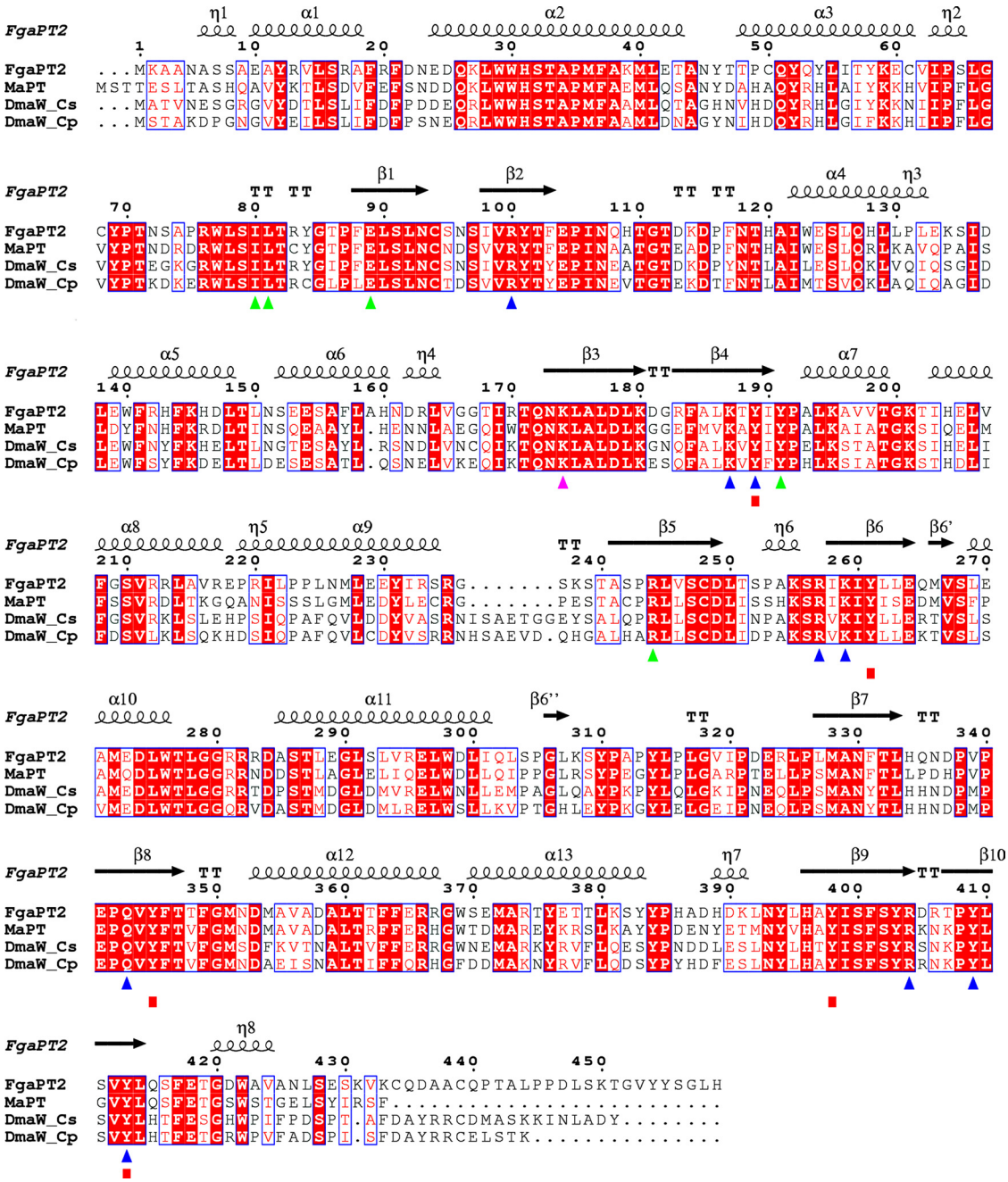


**Fig. S2.** Alignment of the fungal DMATS FgaPT2, MaPT, DmaW_Cs, and DmaW_Cp. The amino acids of FgaPT2 involved in the coordination of the pyrophosphate moiety (▲ = R100, K187, Y189, R257, K259, Q343, R404, Y409, Y413), in the stabilization of the allylic cation via cation-$\pi$ interactions (■ = Y345) by shielding the reactive carbocation (■ = Y189, Y261, Y345, Y398, Y413), in the binding of the aromatic substrate tryptophan (▲ = I80, L81, E89, Y191, R244), and in the abstraction of the proton from the $\sigma$-complex (▲ = K174) are marked with colored symbols. The alignment was created with ESPript 2.2 (12): $\alpha$, $\alpha$-helices; $\eta$, $3_{10}$-helices; $\beta$, $\beta$-strands; TT, strict beta turns. Strict sequence identity is shown by a red box with a white character, and similarity is shown by red characters in a blue frame.

12. Gouet P, Courcelle E, Stuart DI, Metoz F (1999) ESPript: Analysis of multiple sequence alignments in PostScript. *Bioinformatics* 15:305–308.

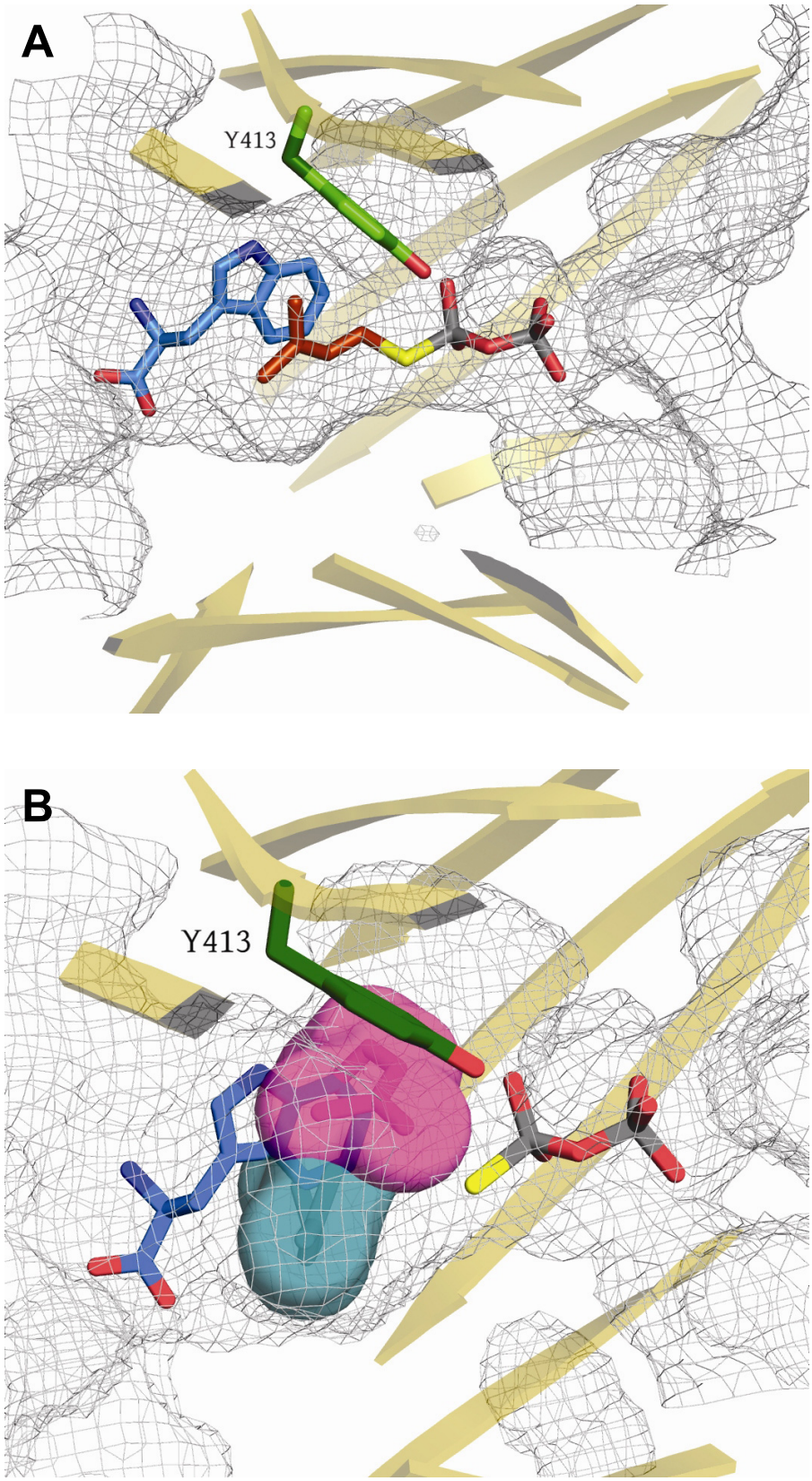


**Fig. S3.** (*A*) Solvent-accessible core of FgaPT2 with both substrates bound. (*B*) Model for dimethylallyl group bound in $\sigma$-transition state to C4 (blue) and C7 (pink) of tryptophan. The dimethylallyl group at C-4 fits well into the solvent-accessible core, but the same group at C-7 would cause steric clashes with Tyr-413. Even more severe steric problems would arise for substitutions at C-5 and C-6.

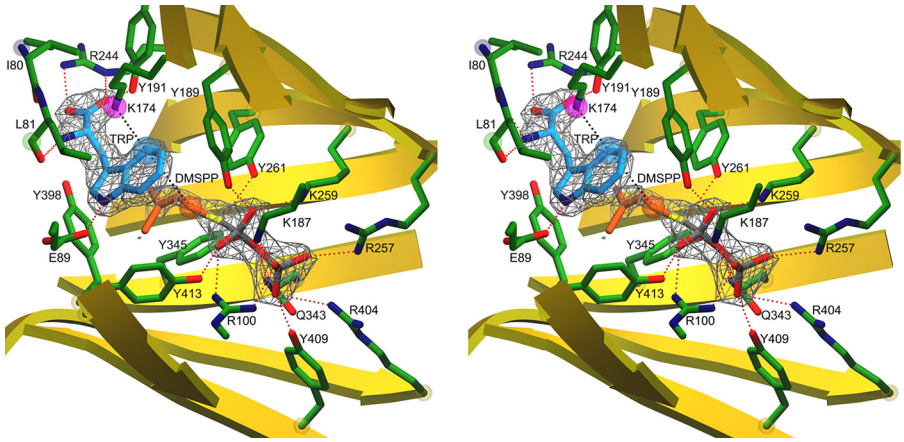


**Fig. S4.** Stereo drawing of the active center of FgaPT2 depicting the omit map (gray) of the substrates tryptophan (blue) and DMSPP (orange) at a $\sigma$-level of 1.5. Hydrogen bonds are shown in red. The reaction center C4 of tryptophan, the electrophilic atom C1′ of DMSPP, and the amino group of K174 are emphasized by blue, orange, and magenta spheres, respectively.

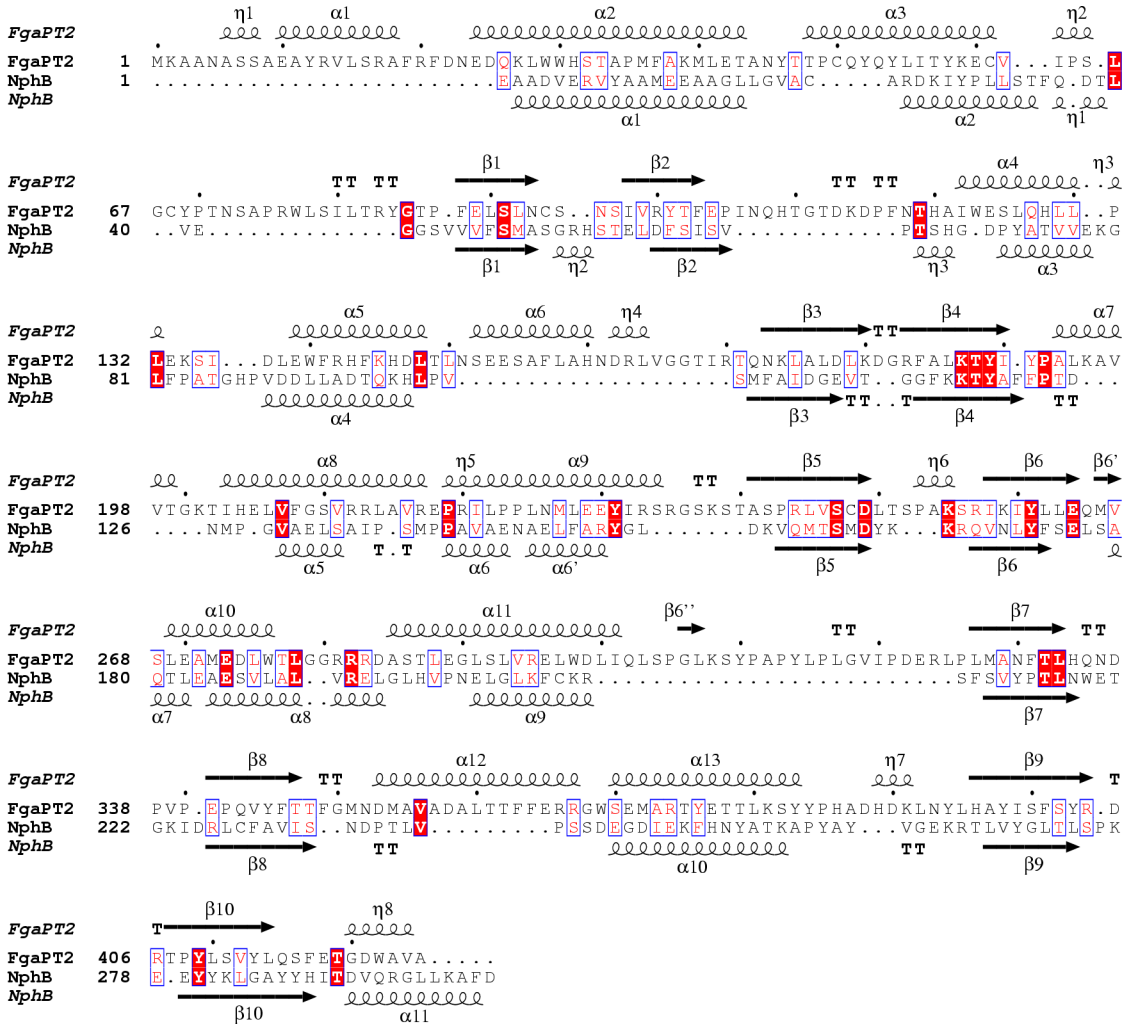


**Fig. S5.** Structure-based alignment of the amino acid sequences of FgaPT2 and NphB. The alignment was created with the SSM program (13) and the layout with ESPript 2.2 (12): $\alpha$, $\alpha$-helices; $\eta$, $3_{10}$-helices; $\beta$, $\beta$-strands; TT, strict $\beta$-turns; TTT, strict $\alpha$-turns. Strict sequence identity is shown by a red box with a white character, and similarity is shown by red characters in a blue frame. The Risler matrix was used with a global score of 0.7.

12. Gouet P, Courcelle E, Stuart DI, Metoz F (1999) ESPript: Analysis of multiple sequence alignments in PostScript. *Bioinformatics* 15:305–308.
13. Krissinel E, Henrick K (2004) Secondary-structure matching (SSM), a new tool for fast protein structure alignment in three dimensions. *Acta Crystallogr D* 60:2256–2268.

**Table S1. Data collection statistics**

| | FgaPT2 | Uranyl nitrate soak | Ternary complex of FgaPT2 |
|---|---|---|---|
| Beamline | ESRF ID 14.4 | Home source | SLS XDA06 |
| Wavelength λ, Å | 0.9395 | 1.54179 | 1.2750 |
| Detector | ADSC Q315r | MAR345 | MAR225 |
| Detector distance, mm | 276.2 | 209.6 | 120.6 |
| Resolution, Å | 25–1.76 (1.80–1.76) | 18.0–2.7 (2.77–2.7) | 30.0–2.08 (2.13–2.08) |
| No. reflections | | | |
| Measured | 644,849 (26,434) | 536,343 (35,581) | 351,121 (24,730) |
| Unique | 98,919 (7,030) | 52,317 (3,746) | 59,060 (4,329) |
| $R_{meas}$, % | 5.6 (59.1) | 14.1 (60.6) | 8.3 (54.6) |
| Completeness, % | 99.7 (96.8) | 99.5 (97.2) | 99.9 (100.0) |
| Multiplicity | 6.5 (3.8) | 10.3 (9.5) | 6.0 (5.7) |
| $<I>/<\sigma(I)>$ | 21.1 (2.9) | 17.5 (4.6) | 17.7 (3.44) |
| Wilson factor, Å$^2$ | 30.1 | 36.1 | 32.4 |
| Crystal mosaicity, ° | 0.15 | 0.30 | 0.32 |

The space group was $P2_12_12_1$ with a dimer in the asymmetric unit.
The solvent content was 51%. Values in parentheses are for the highest shell.
Unit cell parameters were a = 80.1 Å, b = 98.8 Å, c = 125.6 Å; a = 80.4 Å, b = 98.2 Å, c = 125.0 Å; and a = 79.1 Å, b = 97.9 Å, c = 125.1 Å for the native, uranyl derivate, and ternary complexes, respectively.

**Table S2. Refinement statistics**

| | FgaPT2 | Ternary complex of FgaPT2 |
|---|---|---|
| Resolution range, Å | 25–1.76 | 20–2.10 |
| $R_{Cryst}$ | 0.151 | 0.150 |
| $R_{free}$ (test set of 3%) | 0.183 | 0.200 |
| No. non-H atoms (partial occupancy) | | |
| Chain A/chain B/chain N* | 3,637/3,507/101 | 3,460/3,441/23 |
| Glycerol | 4 | 2 |
| 1,3-butanediol | 8 | — |
| Water | 685 | 588 |
| Average isotropic B-factor, Å$^2$ | | |
| Main chain A/B/N* | 21.7/26.9/40.0 | 29.7/33.7/80.0 |
| Side chain A/B/N* | 25.7/31.0/40.3 | 31.9/35.6/72.9 |
| Glycerol | 40 | 38.4 |
| 1,3-butandiol | 41 | |
| Water molecules | 20.3 | 27.2 |
| rmsd for bond lengths, Å | 0.014 | 0.014 |
| rmsd for bond angle, ° | 1.447 | 1.553 |
| Ramachandran regions | | |
| Most favorable, % | 91.1 | 90.7 |
| Allowed, % | 8.9 | 9.3 |
| Outliers, % | — | — |

*Amino acids in chain N belong to C-terminus but cannot be assigned to A- or B-chain